Proceedings of CECNet 2022
A.J. Tallón-Ballesteros (Ed.)

doi:10.3233/FAIA220531

A Lowpass-Bandpass Diplexer Using Common Lumped-Element Dual-Resonance Resonator

Shan JIN
No.38 Research Institute of CETC, Hefei, China

Abstract. A lowpass-bandpass (LP-BP) diplexer with one lowpass channel (LPC) and one bandpass channel (BPC) is presented. The lumped-element dual-resonance resonator as common resonator is proposed to connect inductors, capacitors and *LC* resonator to constitute the desired channels. The LPC design is combined with parameters optimization and the lowpass transformation method, and the BPC design can be developed using the classical design theory of coupled-resonator filter. As an example, a 0.9 / 1.8 GHz LP-BP diplexer is designed and fabricated, which exhibits high return loss (RL), low insertion loss (IL), wide bandwidth (BW), high isolation and extremely compact size.

Keywords. Diplexer, lowpass filter, bandpass filter, lumped element microwave circuits

1. Introduction

Recently, the multiplexers play a very important role in signal synthesis and distribution in modern multi-service and multi-standard communication systems [1~8].

A LP-BP triplexer is proposed in [1], but the defected ground structure increases the installation complexity and may lead to power leakage. In [2], the lowpass channel (LPC) is designed by cascading multiple different sizes of the quasi-elliptic lowpass structure, but its bandpass channels (BPCs) suffer from narrow bandwidths (BWs) and high insertion losses (ILs). Another LP-BP diplexer design approach by using the impedance matching method is reported in [3], but the coupled-line BPC typically is difficult to be realized in the external quality factor due to the line space limitation between the coupled feeding line and coupled-line. Moreover, the above LP-BP multiplexers are mainly based on the distributed-parameter resonators which have a relatively large size.

In this paper, a novel LP-BP diplexer design is proposed by using a common lumped-element dual-resonance resonator, which the electrical performance and circuit size can be improved.

2. 0.9/1.8 GHz LP-BP Diplexer Design

Figure 1(a) shows the circuit model of proposed LP-BP diplexer, and the circuit model of lumped-element dual-resonance resonator and conventional L_bC_b resonator are

Shan Jin, No.38 Research Institute of CETC, Hefei, China; E-mail: 547868509@qq.com.

presented in Figure 1(b) and Figure 1(c) respectively. The L_1C_1 branch of lumped-element dual-resonance resonator together with inductors and capacitors constitute a 5th-order LPC with 3dB cutoff frequency $f_{c\text{-}3dB}$ = 0.9 GHz, and the L_2C_2 branch of lumped-element dual-resonance resonator coupled with a L_bC_b resonator by using a capacitor C_e constitute a second-order BPC with central frequency f_b = 1.8 GHz.

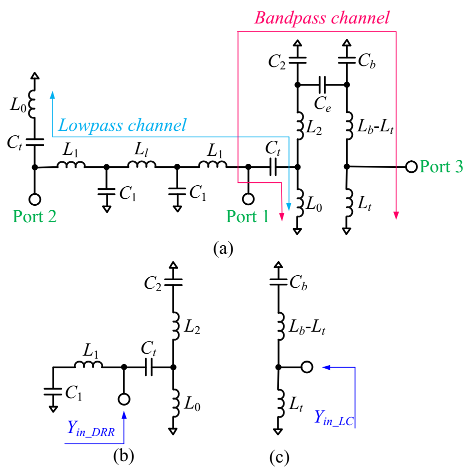

Figure1. Circuit model of (a) proposed LP-BP diplexer, (b) lumped-element dual-resonance resonator proposed in [9], (c) conventional LC resonator.

A. Resonator Analysis

According to the work [9], the input admittance $Y_{in\text{-}DRR}$ of lumped-element dual-resonance resonator can be written as

$$Y_{in\_DRR} = \frac{j\omega\left(p_{N1}\omega^4 + q_{N1}\omega^2 + r_{N1}\right)}{p_{D1}\omega^6 + q_{D1}\omega^4 + r_{D1}\omega^2 + 1} \tag{1}$$

where

$$\omega = 2\pi f \quad p_{N1} = \left[L_0L_2 + \left(L_0 + L_2\right)L_1\right]C_1C_2C_t$$

$$q_{N1} = -\left[\left(L_0 + L_2\right)\left(C_1 + C_t\right)C_2 + \left(L_0 + L_1\right)C_1C_t\right]$$

$$r_{N1} = C_1 + C_t \quad p_{D1} = -L_0L_1L_2C_1C_2C_t$$

$$q_{D1} = \left(L_0 + L_2\right)L_1C_1C_2 + L_0L_1C_1C_t + L_0L_2C_2C_t$$

$$r_{D1} = -\left[\left(L_0 + L_2\right)C_2 + L_0C_t + L_1C_1\right]$$

When $q_{N1}^2 - 4p_{N1}r_{N1} > 0$ is built, its natural resonant frequency with higher frequency f_{DRR2} is given by

$$f_{DRR2} = \frac{1}{2\pi}\sqrt{\frac{-q_{N1} + \sqrt{q_{N1}^2 - 4p_{N1}r_{N1}}}{2p_{N1}}} \tag{2}$$

The external quality factor $Q_{e\text{-}DRR2}$ of lumped-element dual-resonance resonator at f_{DRR2} can be expressed by

$$Q_{e\_DRR2} = Z_0 \pi f_{DRR2} \left. \frac{\partial \left[\mathrm{Im}\left(Y_{in\_DRR} \right) \right]}{\partial f} \right|_{f = f_{DRR2}} \tag{3}$$

where $Z_0 = 50\ \Omega$ is the port impedance.

The input admittance $Y_{in\text{-}LC}$ of L_bC_b resonator can be derived as

$$Y_{in\_LC} = \frac{1 - \omega^2 L_b C_b}{j\omega L_t [1 - \omega^2 (L_b - L_t) C_b]} \tag{4}$$

The natural resonant frequency f_{LC} of L_bC_b resonator is calculated by

$$f_{LC} = \frac{1}{2\pi\sqrt{L_b C_b}} \tag{5}$$

The external quality factor $Q_{e\text{-}b}$ of L_bC_b resonator can be written as

$$Q_{e\_b} = Z_0\, \pi f_b \left. \frac{\partial \left[\mathrm{Im}\left(Y_{in\_LC} \right) \right]}{\partial f} \right|_{f = f_b} \tag{6}$$

B. LP-BP Diplexer Design

Step 1: 0.9 GHz LPC Design. The circuit model of ideal 5th-order lowpass filter (LPF) is shown in Figure 2, and the L_2C_2 branch in Figure 1(a) is not included for analysis simplicity.

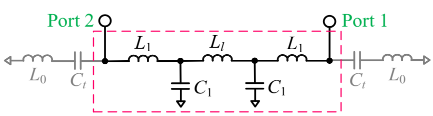

Figure 2. Circuit model of ideal 5th-order LPF.

First of all, the series L_0C_t circuit is temporarily removed from this 5th-order LPF, then the values of L_1, C_1 and L_l are calculated by

$$L_1 = \frac{\Omega_c \gamma_0 g_1}{\omega_c} \tag{7a}$$

$$C_1 = \frac{\Omega_c g_2}{\omega_c \gamma_0} \tag{7b}$$

$$L_l = \frac{\Omega_c \gamma_0 g_3}{\omega_c} \tag{7c}$$

where $\Omega_c = 1$ rad/s, $\gamma_0 = 50$, $\omega_c = 2\pi f_c$, which f_c is the cutoff frequency and $g_{1\sim3}$ are the lumped circuit element values of the lowpass prototype filter referred to [10].This 5th-order LPF is designed for a Chebyshev frequency response and a 28 dB return loss (RL), $f_c = 0.675$ GHz is chosen to acquire $f_{c\text{-}3dB}$ around 0.9 GHz. $L_1 \approx 8.4$ nH, $C_1 \approx 6$ pF and $L_l = 18$ nH can be then derived as using the lowpass transformation method [10]. The frequency response of 5th-order LPF without series L_0C_t circuit is shown in Figure 3 by the dash line.

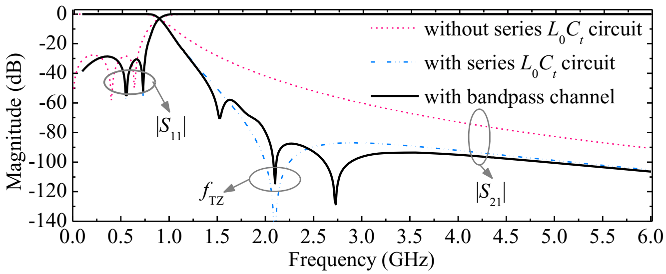

Figure 3. Frequency response of 5th-order LPF with or without series L0Ct circuit, and LPC of LP-BP diplexer.

After the series L_0C_t circuit, which produces the virtual grounds at the connected points is considered in the 5th-order LPF. It will result in a transmission zero (TZ). The frequency location of this TZ f_{TZ} is determined by

$$f_{TZ} = \frac{1}{2\pi\sqrt{L_0 C_t}} \tag{8}$$

C_t = 2.4 pF can be calculated after L_0 = 2.4 nH is preset and f_{TZ} = 2.1 GHz is set in this design. The frequency response of 5th-order LPF is affected by series L_0C_t circuit. It is verified that the values of L_1 and C_1 can be optimized to acquire the desired 5th-order LPF performance. In this design, firstly L_1 = 14.4 nH is selected so that the corresponding return loss (RL) is better than 20 dB within lowpass passband, and then C_1 = 6.6 pF is selected to meet the return loss (RL) requirement of better than 28dB. Interestingly, we find that 3dB cutoff frequency ($f_{c\text{-}3\text{dB}}$) is obtained around 0.9 GHz in the present case. The final frequency response of 5th-order LPF with series L_0C_t circuit is plotted in Figure 3 by the dash-dot line.

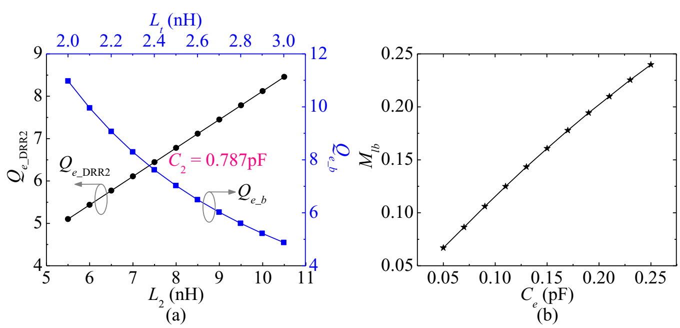

Figure 4. Extracted Q_{e_DRR2}, Q_{e_b} and M_{lb} of lowpass-bandpass diplexer.

Step 2: 1.8 GHz BPC Design. The lumped-element dual-resonance resonator and L_bC_b resonator will build the passband with bandpass response by the coupling capacitor C_e which is actually served as a J-inverter in this case. The ripple bandwidth (RBW) and return loss (RL) of BPC is specified as RBW = 225 MHz and RL = 20 dB. For an ideal second-order BPF, the external quality factor Q_e^{lb} and the coupling coefficients M_{lb} can be acquired as Q_e^{lb} = 6.83 and M_{lb} = 0.12878 [10]. There are various combinations of L_2 and C_2 which can meet the f_{DRR2} = 1.8 GHz. Figure 4(a) shows the extracted Q_{e_DRR2} versus C_2 with fixed f_{DRR2} = 1.8 GHz. L_2 = 8 nH and C_2 = 0.787 pF are calculated to meet Q_e^{lb} = Q_{e_DRR2} and f_b = f_{DRR2}. After C_b = C_2 is preset, L_b = 9.9339nH can be calculated by Eq. (5). The relationship between the variation of $Q_{e\text{-}b}$

and L_t is also shown in Figure 4(a), to meet the condition that $Q_e^{lb} = Q_{e\text{-}b}$, $L_t = 2.54$ nH is chosen. The variation trend of extracted M_{lb} relative to C_e is plotted in Figure 4(b) and $C_e = 0.12$ pF is preselected to acquire the required M_{lb}. In addition, considering the influence of parallel negative capacitances in the *J*-inverter, the design parameters of proposed LP-BP are further optimized. The values of these parameters summarized as $L_0 = 2.4$ nH, $L_1 = 14.4$ nH, $C_1 = 6.6$ pF, $L_l = 18$ nH, $C_t = 2.4$ pF, $L_2 = 8$ nH, $C_2 = C_b = 0.667$ pF, $L_b = 11.1$ nH, $C_e = 0.119$ pF and $L_t = 3$ nH. The solid line in Figure 3 plots the LPC of proposed LP-BP diplexer. It can be observed from Figure 3 that the out-band performance of LPC is improved with extra two TZs introduced by the BPC due to the increased signal transmission paths, and the effect of BPC on LPC is minor beacause the responses of |S11| and |S21| are basically the same with or without BPC.

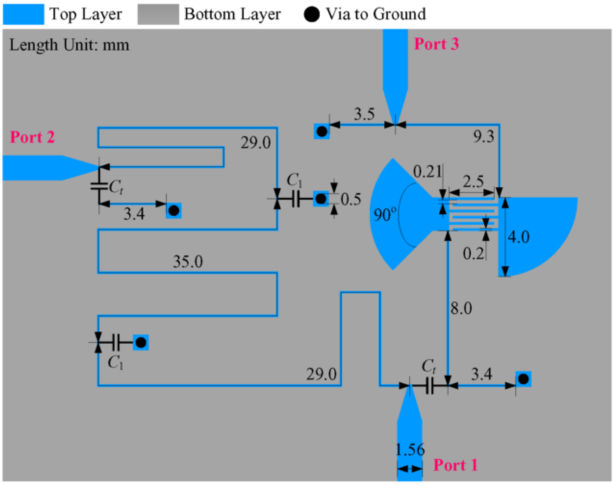

Figure 5. Physical layout of designed LP-BP diplexer (not to scale).

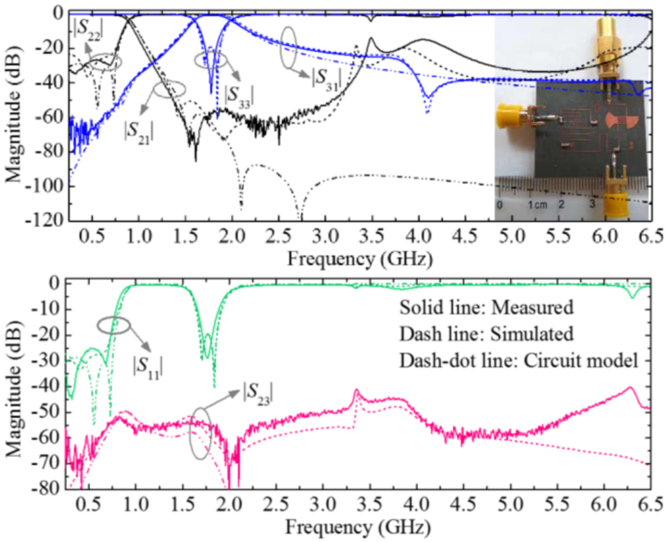

Figure 6. Simulated and measured results of fabricated LP-BP diplexer.

3. Simulated and Measured Results

Figure 5 shows the physical layout of designed LP-BP diplexer. This design was fabricated on a Rogers RT/duroid 5880 substrate, which h = 0.508 mm, ε_{re} = 2.2 and $\tan\delta$ = 0.0009. Its circuit realization approach can refer to the work [11]. Figure 5 also notes the physical dimensions of the final optimization. The illustration is shown in top right of Figure 6 is the photograph of fabricated LP-BP diplexer, it occupies the circuit area of $0.103\times0.063\ \lambda_{gd}^2$ excluding the feeding lines, and the physical dimensions is $34\times21\text{mm}^2$. λ_{gd} is the wavelength of 50 Ω microstrip line at 0.9 GHz on the Rogers RT/duroid 5880 substrate.

Figure 6 plots the simulated and measured results of fabricated LP-BP diplexer. The LPC measured results of 3dB cutoff frequency ($f_{c\text{-}3\text{dB}}$) is 0.87GHz, in-band insertion loss (IL) is 0.3dB, return loss (RL) is better than 20dB. The BPC measured results of central frequency (CF) is 1.78GHz, 3dB fractional bandwidth (FBW) is 20.1%, in-band insertion loss (IL) is 0.65dB, and return loss (RL) is 20dB. The common port return loss (RL) is also better than 20 dB within two passbands, and the isolation between lowpass and bandpass channels are better than 52dB. Table 1 shows a comparison performance between the references [1~3] and this work.

Table 1. Comparison between the references and this work

	[1]	[2]	[3]	This work
fc_3dB and CF (GHz)	1.07/2.45	1.0/1.7	1.5/2.4	0.87/1.78
3dB FBW (%)	7.7	8.5	7.6	20.1
IL of LPC / BPC(dB)	0.8/2.1	0.53/2.08	0.25/2.42	0.3/0.65
Isolation(dB)	40	37	35	52
Circuit size (mm^2)	70×42	74×40	97×62	34×21

4. Conclusion

A 0.9 / 1.8 GHz LP-BP diplexer is presented by using lumped-element dual-resonance resonator and *LC* resonator, and the design procedures are introduced in detail. The proposed LP-BP diplexer exhibits high return loss (RL), insertion loss (IL), high isolation and compact circuit size. Owing to these excellent electrical performances, the proposed structure has a bright prospect in the fields of signal synthesis and distribution.

References

[1] Chen FC, Qiu JM, Hu HT, Chu QX, Michael JL. Design of microstrip lowpass-bandpass triplexer with high isolation. IEEE Microwave and Wireless Components Letters, 2015 Dec; 25(12):805-7.

[2] Tu WH, Wu CL. Design of microstrip low-pass-bandpass multiplexers using distributed coupling technique. IEEE Transactions Components, Packaging and Manufacturing Technology, 2016 Nov; 06(11):1648-1655.

[3] Deng PH, Tsai JT. Design of microstrip lowpass-bandpass diplexer. IEEE Microwave and Wireless Components Letters, 2013 Jul; 23(7):332-4.

[4] Yang T, Chi PL, Itoh T. High isolation and compact diplexer using the hybrid resonators. IEEE Microwave and Wireless Components Letters, 2010 Oct; 20(10):551-553.

[5] Chen CF, Huang TY, Chou CP, Wu RB. Microstrip diplexers design with common resonator sections for compact size, but high Isolation. IEEE Transactions on Microwave Theory and Techniques, 2006 May; 54(5):1945-1952.

[6] Zeng SJ, Wu JY, Tu WH. Compact and high-isolation quadruplexer using distributed coupling technique. IEEE Microwave and Wireless Components Letters, 2011 Apr; 21(4):197-199.
[7] Carceller C, Soto P, Boria V, Guglielmi M, Gil J. Design of compact wideband manifold-coupled multiplexers. IEEE Transactions on Microwave Theory and Techniques, 2015 Oct; 63(10):3398-3407.
[8] Wu JY, Hsu KW, Tseng YH, Tu WH. High-isolation microstrip triplexer using multiple-mode resonators. IEEE Microwave and Wireless Components Letters, 2012 Apr; 22(4):173-175.
[9] Xu J, Wu W, Wei G. Novel dual-band bandpass filter and reconfigurable filters using lumped-element dual-resonance resonators. IEEE Transactions on Microwave Theory and Techniques, 2016 May; 64(5):1496-1507.
[10] Hong JS, Michael JL. Microstrip Filters for RF/Microwave Applications. New York: Wiley, 2001.
[11] Bahl IJ. Lumped Elements for RF and Microwave Circuits. Boston: Artech House, 2003.